

Imaging with terahertz waves

B. B. Hu and M. C. Nuss

AT&T Bell Laboratories, 101 Crawfords Corner Road, Holmdel, New Jersey 07733-3030

Received May 11, 1995

We present what is to our knowledge the first imaging system based on optoelectronic terahertz time-domain spectroscopy. Terahertz time-domain waveforms are downconverted from the terahertz to the kilohertz frequency range, and the waveform for each pixel is frequency analyzed in real time with a digital signal processor to extract compositional information at that point. We demonstrate applications to package inspection and chemical content mapping in biological objects. © 1995 Optical Society of America

Optoelectronic terahertz time-domain spectroscopy (THz-TDS) has come a long way since the first demonstration of free-space THz transmitters and detectors a few years ago.¹ In particular, it has proven to be a powerful tool for spectroscopic measurement of far-infrared properties of materials such as dielectrics and semiconductors,² superconductors,³ liquids,⁴ and gases.⁵ Unlike in traditional Fourier-transform far-infrared spectroscopy, in which a blackbody radiation source and a bolometer are used, both the generation and the detection are optically gated in THz-TDS. This offers extraordinary noise rejection, and signal-to-noise ratios as high as 10,000:1 are achieved.⁶ Also, the detection is coherent—both the amplitude and the phase of the THz waveform are measured, allowing one to extract the full complex dielectric constant of the material under investigation without having to resort to the Kramers–Kronig relations. In general, most chemical compounds show very strong, highly specific frequency-dependent absorption and dispersion in the THz range. This is particularly true for gases that have characteristic narrow absorption lines in this range. But liquids and solids also have rather specific frequency-dependent absorption and dispersion characteristics in this frequency range, leading to characteristic time-domain waveforms when THz radiation passes through different materials. Accordingly, it should be feasible to a certain degree to apply THz-TDS to determine the chemical content of an unknown object. Together with the ability to collimate and focus THz waves down to the diffraction limit of a few hundred micrometers at the sample,⁷ imaging of chemical compositions should be possible with reasonable spatial resolution by the THz-TDS technique. However, until now, acquisition of THz waveforms has required lock-in detection and low-pass filtering with a 100–300-ms time constant per data point. With resulting acquisition times of a few minutes for a single THz waveform at each image point, imaging with THz transients has so far been impractical.

In this Letter we demonstrate practical terahertz imaging for what is to our knowledge the first time. THz transients are focused to a diffraction-limited spot on the sample, and the transmitted THz waveforms are acquired and processed in real time at each point of the sample while the sample is scanned in x and y

at a rate of currently 10–20 pixels/s. We analyze the temporal waveform transmitted through the sample at every pixel of the object in real time, from which information on the chemical composition of the sample can be inferred in many cases. This new application of THz-TDS is permitted by the following advances in the technology: (i) a reduction of the acquisition time for each THz waveform from minutes down to less than 5 ms with a signal-to-noise ratio of still more than 100:1, (ii) downconversion of the THz waveforms into the audio (kilohertz) range with a scanning delay line, and (iii) real-time acquisition, processing, frequency analysis and display of the spectral data of the THz transients by a digital signal processor (DSP). As first examples of this novel technology, we show that this system can be used for safe terahertz-ray (T-ray) package inspection, chemical content mapping, and food inspection.

Figure 1 shows a schematic setup of the THz imaging system. An Ar-ion-pumped self-mode-locked Ti:sapphire laser delivering pulses of 100-fs duration at $\lambda = 800$ nm is used as a femtosecond optical source. Roughly 80 mW from this source is used to excite a THz transmitter. This photoconducting transmitter consists of two strip lines spaced by 50 μm that are lithographically defined on a semi-insulating GaAs substrate, with a bias of 80–100 V applied to the strip lines. In our initial experiment, the imaging optics consists of two pairs of off-axis paraboloid reflectors. The THz radiation from the transmitter is first collimated and then focused down to a diffraction-limited spot on the object by the first pair of paraboloids, and another pair of paraboloids is used to collect and focus the THz radiation from the sample onto the optically gated THz dipole detector. The detector is a 50- μm -wide radiation-damaged silicon-on-sapphire photoconducting dipole antenna with a 5- μm gap.¹ The THz detector is optically gated by approximately 60 mW of the laser beam. Both the transmitter and the receivers have high-resistivity silicon hyperhemispherical substrate lenses attached to the backs of their substrates to improve coupling of the THz radiation to air. A 20-Hz scanning delay line temporally downconverts the THz waveforms into the audio (kilohertz) range, with the downconversion ratio given by twice the ratio of the speed of the delay line to the speed of light. In our example the scanning

delay line with a speed of 15 cm/s converts a 1-THz waveform exactly to a 1-kHz waveform. The amplitude of the scan is approximately 0.75 cm, resulting in a spectral resolution of 20 GHz. The signal is then amplified by a current preamplifier, digitized, and processed by the DSP on the flight for each pixel. Both the analog-to-digital (A/D) converter and the DSP are integrated on a commercial signal processing board (Data Translation DT3818). The spectral information at each pixel is obtained and processed by the board in less than 5 ms. The typical real-time THz signal has an amplitude of 10 V after passing the 10^9 V/A current preamplifier with a signal-to-noise ratio of greater than 100:1. In this first implementation of the THz imaging experiment, the sample, rather than the THz beams, is scanned. Currently the THz image is acquired, analyzed, and displayed at a rate of 12 pixels/s. Simple modifications are expected to increase this rate into the neighborhood of 100 pixels/s, so that a 100×100 image can be obtained in little over a minute.

As a first application we demonstrate the use of this novel technique for industrial inspection. In a manner similar to x-ray inspection, an image is formed from the differences in transmittance through different materials inside a concealed package. However, unlike x-ray inspection, our T-ray technique is safe, nondestructive, and free of hazardous effects and can therefore potentially provide an alternative solution for security checking, package inspection, etc. Plate I shows a THz image of a semiconductor integrated-circuit chip package. The THz image contains 50,000 pixels, and the THz transmission is color coded according to the total intensity of the transmitted THz signal integrated over a 1–3-THz frequency range. The plastic packaging material of the chip shows only little absorption in the THz spectral range, whereas metals are fully absorbing and doped semiconductors are partially absorbing.² Hence, the image clearly shows the silicon chip area as well as the metal leads connecting to the package pins. A spatial resolution of roughly $250 \mu\text{m}$

is achieved. Even better spatial resolution can be obtained by having the DSP process only higher THz frequencies, of course at the expense of signal strength.

Another application of the T-ray imaging technique is to detect and map out chemical compositions within an object. To demonstrate this application, we apply this technique to obtain the water distribution within a leaf. The water content inside the leaf causes strong absorption of THz light in the high-frequency range (>500 GHz). To map out the water content of the leaf, we compare the amplitude spectrum of the THz signal passing through the leaf with the reference spectrum without the sample by the DSP. For a leaf approximately $4.5 \text{ cm} \times 2.3 \text{ cm}$, spectral information at 30,000 pixels is recorded with a spatial resolution of roughly $400 \mu\text{m}$. Plate II shows a THz image of a fresh leaf (left) and a THz image of the same leaf after 48 h (right). Also shown at the right is a color scale for the relative water concentration. Although the visible appearance of the leaf (not shown) does not change appreciably within this time span, the THz image shows a very prominent change, indicating that the water distribution has changed dramatically over 48 h as the water has gradually evaporated from the leaf. In particular, we see that water has largely disappeared from the bulk of the leaf, whereas appreciable water content still remains in the stems of the leaf.

Similar measurements have also been successfully performed on a variety of other samples. For example, meat absorbs THz radiation because of its moisture content, whereas fat is nearly transparent to THz radiation. Thus from a THz image of a piece of bacon we are able to map out the fat distribution, indicating some possible applications to food inspection. This technology could also be extended to medical tissue and biomedical studies, for example, for skin cancer detection, as the water retention of tumors may be different from that for healthy tissue. We can also see the technology potentially applied to gas monitoring and industrial process control, such as in a combustion chamber or in a reactive-ion etcher. The

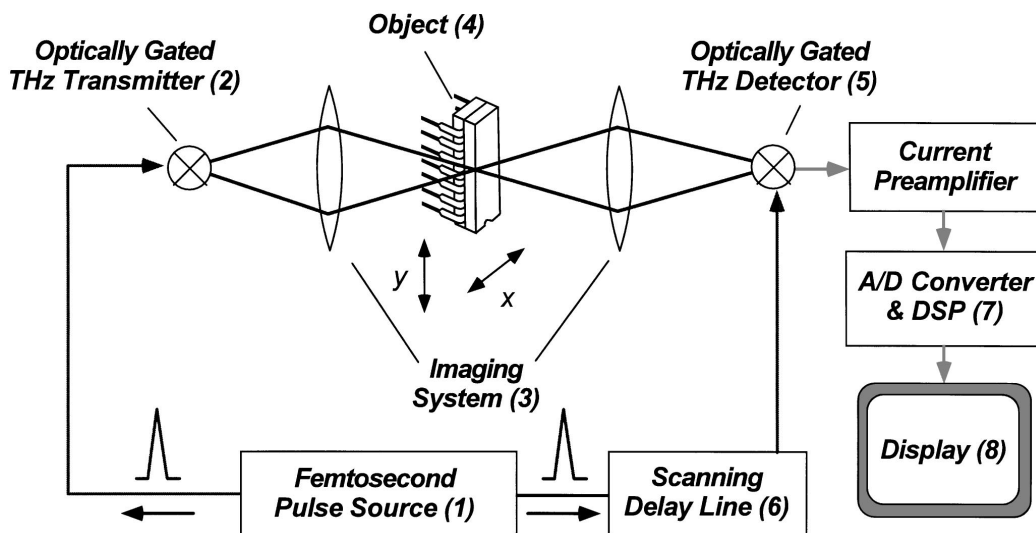


Fig. 1. Schematic of the THz imaging system. In our experiments the object is raster scanned by a two-axis motorized stage.

latter application can be very specific to the chemical composition, as gases have unique and narrow spectral absorption lines, leading to oscillations in the THz waveforms that can easily be picked up by a DSP.

There are also some technical aspects of the T-ray imaging system that merit some discussion. Currently, only the magnitude of the THz spectrum is obtained and extracted from the THz waveform at each image pixel with the numerical fast-Fourier-transform function of the DSP. An obvious future improvement of the T-ray imaging technology will include the use of speech recognition algorithms⁸ for recognition of the THz waveforms in amplitude and phase. We anticipate that this will allow one to extract chemical compositions more reliably even in the solid and liquid phases, where no sharp spectral absorption lines are present. Also, in this preliminary demonstration the sample rather than the THz beam is scanned. In future implementations the THz beam could be scanned across the sample instead. Alternatively, an array of THz detectors could be designed to acquire the entire image at once. With current microelectronics fabrication technology, one should be able to fabricate a 100×100 focal-plane array of photoconducting dipole antennas to replace the single dipole detector that we used. Last but not least, we need to emphasize that, although this experiment was still performed with an Ar-ion-pumped Ti:sapphire laser, our technique will become realistic and practical with compact, cost-effective, and plug-efficient femtosecond laser sources,⁹ which will soon become commercially available for real-world applications of this and other short-pulse laser applications.

In summary, we have demonstrated a novel chemical imaging system based on optoelectronic terahertz time-domain spectroscopy. We show that this system can be applied to safe T-ray package inspection and chemical content mapping. This system should have many applications, such as industrial process control, medical tissue diagnosis, food inspection, biological and biomedical imaging, and environmental monitoring.

References

1. P. R. Smith, D. H. Auston, and M. C. Nuss, *IEEE J. Quantum Electron.* **24**, 255 (1988).
2. D. Grischkowsky, S. Keiding, M. van Exter, and C. Fattering, *J. Opt. Soc. Am. B* **7**, 2006 (1990).
3. M. C. Nuss, P. M. Mankiewich, M. L. O'Malley, E. H. Westerwick, and P. B. Littlewood, *Phys. Rev. Lett.* **66**, 3305 (1991).
4. J. E. Pedersen and S. Keiding, *IEEE J. Quantum Electron.* **28**, 2518 (1992).
5. H. Harde and D. Grischkowsky, *J. Opt. Soc. Am. B* **8**, 1642 (1991).
6. M. van Exter and D. Grischkowsky, *IEEE Microwave Theory Technol.* **38**, 1684 (1990).
7. M. C. Nuss, K. W. Goossen, J. P. Gordon, P. M. Mankiewich, M. L. O'Malley, and M. Bhushan, *J. Appl. Phys.* **70**, 2238 (1991).
8. L. R. Rabbiner and B. H. Juang, *Fundamentals of Speech Recognition* (Prentice-Hall, Englewood Cliffs, N.J., 1994).
9. D. Kopf, K. J. Weingarten, L. R. Brovelli, M. Kamp, and U. Keller, *Opt. Lett.* **19**, 2143 (1994); S. Tsuda, W. H. Knox, E. A. de Souza, W. Y. Jan, and J. E. Cunningham, *Opt. Lett.* **20**, 1406 (1995).

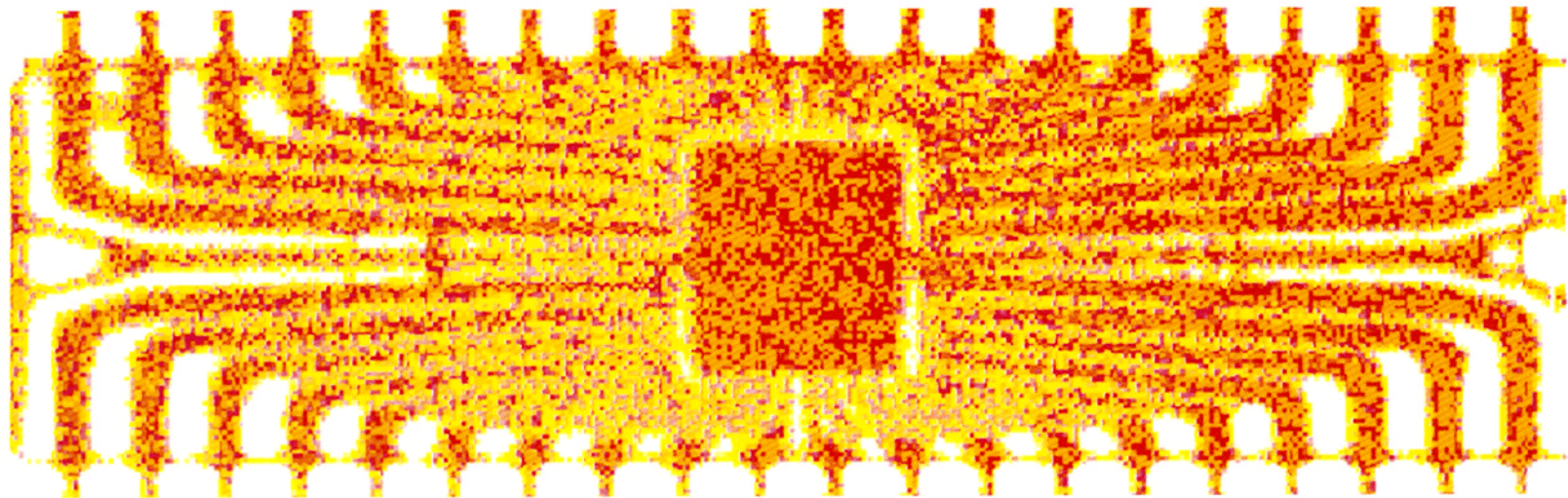


Plate I. THz image of a packaged semiconductor integrated circuit (plastic packaging).

